

# Methods of analysis of Chloroplast Genomes of C3, Kranz type C4 and Single Cell C4 photosynthetic members of Chenopodiaceae

**Richard Sharpe**

Washington State University Department of Horticulture

**Bruce Andreas Williamson-Benavides**

Washington State University Department of Horticulture

**Gerry Edwards**

Washington State University

**Amit Dhingra** (✉ [adhingra@wsu.edu](mailto:adhingra@wsu.edu))

Washington State University <https://orcid.org/0000-0002-4464-2502>

---

## Research

**Keywords:** Chenopodiaceae, chloroplast genome, Single Cell C4 photosynthesis, genomics, Amaranthaceae

**Posted Date:** August 10th, 2020

**DOI:** <https://doi.org/10.21203/rs.3.rs-27622/v2>

**License:**  This work is licensed under a Creative Commons Attribution 4.0 International License.

[Read Full License](#)

---

**Version of Record:** A version of this preprint was published on August 31st, 2020. See the published version at <https://doi.org/10.1186/s13007-020-00662-w>.

# Abstract

**Background** Chloroplast genome information is critical to understanding forms of photosynthesis in the plant kingdom. During the evolutionary process, plants have developed different photosynthetic strategies that are accompanied by complementary biochemical and anatomical features. Members of family Chenopodiaceae have species with C<sub>3</sub> photosynthesis, and variations of C<sub>4</sub> photosynthesis in which photorespiration is reduced by concentrating CO<sub>2</sub> around Rubisco through dual coordinated functioning of dimorphic chloroplasts. Among dicots, the family has the largest number of C<sub>4</sub> species, and greatest structural and biochemical diversity in forms of C<sub>4</sub> including the canonical dual-cell Kranz anatomy, and the recently identified single cell C<sub>4</sub> with the presence of dimorphic chloroplasts separated by a vacuole. This is the first comparative analysis of chloroplast genomes in species representative of photosynthetic types in the family.

**Results** Methodology with high throughput sequencing complemented with Sanger sequencing of selected loci provided high quality and complete chloroplast genomes of seven species in the family and one species in the closely related Amaranthaceae family, representing C<sub>3</sub>, Kranz type C<sub>4</sub> and single cell C<sub>4</sub> (SSC<sub>4</sub>) photosynthesis. Six of the eight chloroplast genomes are new, while two are improved versions of previously published genomes. The depth of coverage obtained using high-throughput sequencing complemented with targeted resequencing of certain loci enabled superior resolution of the border junctions, directionality and repeat region sequences. Comparison of the chloroplast genomes with previously sequenced plastid genomes revealed similar genome organization, gene order and content with a few revisions. High-quality complete chloroplast genome sequences resulted in correcting the orientation the LSC region of the published *Bienertia sinuspersici* chloroplast genome, identification of stop codons in the *rpl23* gene in *B. sinuspersici* and *B. cycloptera*, and identifying an instance of IR expansion in the *Haloxylon ammodendron* inverted repeat sequence. The rare observation of a mitochondria-to-chloroplast inter-organellar gene transfer event was identified in family Chenopodiaceae.

**Conclusions** This study reports complete chloroplast genomes from seven Chenopodiaceae and one Amaranthaceae species. The depth of coverage obtained using high-throughput sequencing complemented with targeted resequencing of certain loci enabled superior resolution of the border junctions, directionality, and repeat region sequences. Therefore, the use of high throughput and Sanger sequencing, in a hybrid method, reaffirms to be rapid, efficient, and reliable for chloroplast genome sequencing.

# Introduction

Plastids convert light energy into chemical energy and are an essential site for the biosynthesis of pigments, lipids, several amino acids and vitamins [1,2]. Comparative genomics studies have facilitated the understanding of chloroplast genome organization and phylogenetic relationships [3–5]. Additionally, availability of chloroplast genome sequences can be useful for constructing transformation vectors to enable chloroplast transformation via homologous recombination [6,7].

Higher plant chloroplast genomes possess a characteristic organization comprising a Large Single Copy (LSC), a Small Single Copy (SSC) and two Inverted Repeat (IRa and IRb) regions, with only a few exceptions, e.g. in *Pisum sativum* and some other legumes [8–10]. Several methods have been used to sequence chloroplast genomes in plants, including primer walking [11–14] and high-throughput sequencing (HTS) [15]. HTS, both with isolated chloroplast DNA [16–18] and total cellular DNA [19–21], has been employed to generate physical maps of the chloroplast genome. However, the junctions of LSC/IRa, IRa/SSC, SSC/IRb and IRb/LSC need to be resolved using additional experimentation [22]. Genome sequencing and subsequent assembly of the chloroplast genome can be challenging due to variable IR borders; presence of chloroplast genome sequences in the nuclear genome; sequence homology between chloroplast and mitochondrial genes, such as the NAD(P)H and NADH dehydrogenase genes; as well as the NAD(P)H genes being distributed throughout the chloroplast genome [3,23–28].

Chloroplasts, the green plastids in plants, are the site for photosynthesis where Ribulose-1,5-bisphosphate carboxylase/oxygenase (Rubisco), captures CO<sub>2</sub> with synthesis of 3-phosphoglyceric acid (3PGA) in the Calvin-Benson cycle, leading to the synthesis of carbohydrates, and cellular constituents. Three major types of oxygenic photosynthesis are known to date: C<sub>3</sub>, C<sub>4</sub>, and Crassulacean acid metabolism (CAM). In C<sub>3</sub> plants, Rubisco directly fixes atmospheric CO<sub>2</sub> introducing carbon into the Calvin-Benson cycle. In C<sub>4</sub> and CAM photosynthesis, CO<sub>2</sub> is first captured by phosphoenolpyruvate carboxylase (PEPC) with synthesis of 4-carbon organic acids which are sequestered in a spatial manner in C<sub>4</sub> plants and a temporal manner in CAM plants. Decarboxylation of the 4-carbon organic acid generates a CO<sub>2</sub>-rich environment around Rubisco [29]. This mechanism suppresses the oxygenation reaction by Rubisco and the subsequent energetically-wasteful photorespiratory pathway. C<sub>4</sub> plants function with spatial separation of two types of chloroplasts, one type supports the fixation of atmospheric CO<sub>2</sub> by PEPC and synthesis of C<sub>4</sub> acids, while the other type utilizes the CO<sub>2</sub> generated from decarboxylation of C<sub>4</sub> acids in the Calvin Benson cycle. In Kranz type C<sub>4</sub> plants mesophyll chloroplasts support fixation of atmospheric CO<sub>2</sub> by PEPC, while bundle sheath chloroplasts utilize CO<sub>2</sub> generated by decarboxylation of C<sub>4</sub> acids. The unique single-cell C<sub>4</sub> (SCC<sub>4</sub>) plants perform C<sub>4</sub> photosynthesis within individual chlorenchyma cells with spatial separation of two types of chloroplasts. One type supports capture of atmospheric CO<sub>2</sub> by PEPC and the other assimilates the CO<sub>2</sub> generated by decarboxylation of C<sub>4</sub> acids in the Benson-Calvin cycle [30–32].

Among dicot families, the Chenopodiaceae and Amaranthaceae families have by far the largest number (~800) of C<sub>4</sub> species, with up to 15 distinct lineages [33]. Although they are currently recognized as separate families in a clade, they are known to be closely related [34]. Chenopodiaceae species are acclimated to diverse ecosystems from xeric to more temperate salt marshes, including highly saline soils; while *Amaranthus* species predominantly occur in tropical and subtropical regions. The Chenopodiaceae family is very diverse, with six structural forms of Kranz anatomy present among its members [35]. Furthermore, it is the only family known to have SCC<sub>4</sub> species [34]. Phylogenetic analyses have identified independent origins of C<sub>4</sub> photosynthesis. In particular, the results allude to the unique

independent origins of C<sub>4</sub> in subfamily Suaedoideae, including Kranz C<sub>4</sub> anatomy in *Suaeda* species and two independent origins of the SCC<sub>4</sub> system in *Bienertia* and *Suaeda* [33,36–39]. In general the causation of these independent events is hypothesized to be a result of the harsh environments induced by global climate change and periodic reductions in CO<sub>2</sub> content over the past 35 million years [40,41].

In this study, complete chloroplast genome sequences for seven Chenopodiaceae species and one Amaranthaceae species were generated using whole leaf tissue genomic DNA (gDNA) via HTS complemented with Sanger sequencing of targeted loci. The species analyzed were: *Bassia muricata* (C<sub>4</sub>-Kochioid anatomy, tribe Camphorosmoideae), *Haloxylon ammodendron* (C<sub>4</sub>-Salsoloid anatomy, tribe Salsoleae), *Bienertia cycloptera* (C<sub>4</sub>: SCC<sub>4</sub>-tribe Suaedeae), *Bienertia sinuspersici* (C<sub>4</sub>: SCC<sub>4</sub>-tribe Suaedeae), *Suaeda aralocaspica* (SCC<sub>4</sub>-tribe Suaedeae), *Suaeda eltonica* (C<sub>4</sub>-Schoberoid type anatomy, tribe Suaedeae), and *Suaeda maritima* (C<sub>3</sub>-tribe Suaedeae). The chloroplast genome from *Amaranthus retroflexus* (C<sub>4</sub>-Atriplicoid type anatomy, family Amaranthaceae, tribe Amarantheae), was also sequenced and used for comparative analysis. These dicot species include representative species having C<sub>3</sub>-type photosynthesis with monomorphic chloroplasts, and C<sub>4</sub> species having dimorphic chloroplasts for C<sub>4</sub> function including its development in Kranz anatomy versus individual chlorenchyma cells. The purpose of the present study was to determine among these representative dicot species whether the chloroplast genomes between C<sub>3</sub> and C<sub>4</sub> species, and the chloroplast genomes between the various forms of C<sub>4</sub>, are highly conserved (in size and composition), and the degree of difference between the species.

## Results And Discussion

### Genome sequencing and assembly

A summary of the sequencing data obtained from Illumina sequencing and assembly of *A. retroflexus*, *B. muricata*, *B. cycloptera*, *B. sinuspersici*, *H. ammodendron*, *S. aralocaspica*, *S. eltonica*, and *S. maritima* chloroplast genomes is presented in Table 1. Three large contigs with overlapping 5' and 3' regions were generated during genome assembly for *A. retroflexus*, *B. muricata*, *B. cycloptera*, *B. sinuspersici*, *H. ammodendron*, *S. aralocaspica*, and *S. maritima*. These three contigs were identified as LSC, SSC, and IR via BLAST homology alignment [42], GE-Seq - Annotation of Organellar Genomes [43] and DOGMA gene identity prediction [44]. The overlapping regions were present at all four possible junctions when the IR region was reverse complemented (LSC-IR, IR-SSC, SSC-IR, and IR-LSC). These overlapping areas ranged from 19 to 51 nt (illustrated in Fig. S1 with *B. cycloptera*). The directionality of the LSC, SSC and IR, and all overlapping aligned junctions were validated via Sanger sequencing of both strands of the amplicons generated from these regions (Table S1; Fig. S1). For *S. eltonica*, the LSC-IRa and IRb-LSC overlapping regions were 23 nt long and were validated with Sanger sequencing (Table S1). The IRa-SSC and SSC-IRb sections were both missing a 1,475 nt section in the IRa and IRb borders. The 300 nt sequence contiguous to the 1,475 nt section had a low GC content of 19%. A possible cause of the shortened contig flanking the IR-1475 area may be due to the low GC content value which could impact the accuracy of the

HTS genome assembly [45]. The 1,475 nt section was sequenced by primer walking and Sanger sequencing (Table S1). The GC content in the 1,475 nt region and IR was 31.3% and 42.1%, respectively.

The average base depth of coverage for the eight assembled chloroplast genomes ranged from 1553 to 5998-fold. For accurate assembly a minimum of 30-40x sequence coverage is recommended [46–48]. In this study, the only areas with less than 40x average coverage were identified in the last 1 to 3 nucleotides of the IRb sequence for each of the eight genomes. This is expected due to the assembler algorithm parameters. The end of the IRb and the beginning of the LSC were concatenated and these sections were remapped. Remapped coverage results were reported to be above 40x for the IRb ends and surrounding areas. The eight assembled genomes (0.8/0.9 for the read length fraction/similarity fraction mapping) were also compared with a more stringent remapping of the reads to the contigs of 0.99/0.99 length fraction/similarity fraction. Analyses with both levels of stringency show almost identical assembly minimum-coverage and average-coverage for the eight species sequenced in this study (Fig. S2).

Overall, the assembly and subsequent Sanger sequencing-based validation generated high quality and complete chloroplast genomes with all possessing a quadripartite structure as reported in other land plant species.

### **Size, organization and gene content of the chloroplast genomes**

The size of the chloroplast genomes from the eight species ranged from 146,634 to 161,251 nt (Table 2). As expected, each chloroplast genome included a pair of inverted repeat regions, IRa and IRb, separated by an SSC and an LSC region (Table 2 and Fig. S3). With one exception, the size of the IRs ranged from 23,461 to 25,213 nt. (Table 2). The *H. ammodendron* inverted repeat sequence presented an instance of IR length expansion (29,061 nt) compared to the other seven species. The GC content was similar among the eight species and for all the plastomes, LSC, SSC and IRs it ranged from 36.4-36.6, 34.1-34.6, 29.1-30.2 and 42.1-43.0%, respectively (Table 2). All chloroplast genomes contained a similar number of protein coding, ribosomal, and tRNA genes. The number of genes and tRNAs ranged from 113 to 116 and 27-29, respectively in the eight genomes (Table 3 and Fig. S3). For seven out of eight species, 60.1-61.9% of the chloroplast sequence consisted of coding region, which included 52.7-54.3% of protein coding genes and 7.4-7.9% of RNA genes. The *S. eltonica* chloroplast genome was composed of 56.8% coding region including 48.9% of protein coding genes and 7.9% of RNA genes. This difference between *S. eltonica* and the rest of chloroplast genomes is possibly due to the higher repeat content in intergenic sequences of the *S. eltonica* chloroplast genome (Table 4 and Fig. 1).

Gene order and content were largely conserved among the eight chloroplast genomes in this study. However, some structural rearrangements, gene losses and IR expansions were identified. The genes *ycf15*, *ycf68*, and *rpl23* were identified as pseudogenes due to the presence of internal stop codons. The *ycf15* and *ycf68* genes are quite commonly classified as pseudogenes in angiosperms [23,49]. The *rpl23* is also classified as a pseudogene in some species such as the *Fagopyrum* spp., buckwheat, and spinach as well as *Suaeda* and *Haloxylon* species [22,23,50,51]. In *S. eltonica*, *rpl23* was not predicted to be in the chloroplast genome by GeSeq but it was identified as a pseudogene via the BLAST sequence analysis

[42]. No stop codons were identified in the rpl23 of a previously published *B. sinuspersici* chloroplast genome [52]. In this study, 4 stop codons were identified at the same locations for *B. sinuspersici* and its close relative *B. cycloptera*.

At least one complete copy of the ycf1 gene was identified in the eight chloroplast genomes (total length of 5.3-5.6 Kb). In seven out of the eight chloroplast genomes, a duplicated ycf1 pseudogene (1,000-1,300 nt) was found at the IRa-SSC boundary. This is a common feature found in other species [23,53]. In the case of *H. ammodendron*, there is a complete duplication of the ycf1 gene, therefore the *H. ammodendron* chloroplast genome has two full copies in the IR-SSC borders. The complete duplication of the ycf1 gene in *H. ammodendron* leads to the previously mentioned IR expansion (Fig. S3). This phenomenon has also been observed in *Amphilophium*, *Adenocalymma*, *Anemopaegma*, and *Fagopyrum* species; these species possess an expanded IR region and two full-length copies of ycf1 gene [23,54,55]. The IRs for the other seven species are variable in length. In *A. retroflexus*, *B. muricata*, *B. cycloptera*, *B. sinuspersici*, *S. aralocaspica* and *S. maritima*, the IR includes the duplicated ycf1 pseudogene (1-1.3 kb) (Fig. S3). A small segment of the ycf1 gene is also duplicated in *V. vinifera*, *S. oleracea* and *B. vulgaris*. In *S. eltonica*, the IR has expanded to include the trnH-GTG and a fragment of the psbA gene (Fig. S3). The biological significance of this duplication remains unknown.

Annotation of the ycf15 gene with the Dual Organellar Genome Annotator (DOGMA) [44] shows variability in terms of its physical location. In *A. retroflexus*, *B. vulgaris* and *S. eltonica*, the ycf15 is located between the rps12 and trnV-GAC. In *B. cycloptera*, *B. muricata*, *B. sinuspersici*, *H. ammodendron*, *S. aralocaspica*, and *S. maritima* the ycf15 is located between ycf2 and trnL-CAA. The ycf15 as well as other genes, such as the ycf2, psbA, clpP, and matK, have been reported to have variable physical location in different plants [56–59].

The genes ycf3, clpP, rpoC1, and rpl2 have been found to have a variable number of introns among and within some taxonomic groups [23]. The gain or loss of introns in these genes have occurred independently in several lineages of flowering plants [23,60]. However, no differences were found in the number of introns among the eight species; the ycf3, clpP, rpoC1, and rpl2 contain 2, 2, 1, and 0 introns, respectively.

The orientation of the SSC region in *A. retroflexus*, and *B. muricata* differs from the orientation of the SSC in *B. cycloptera*, *B. sinuspersici*, *H. ammodendron*, *S. aralocaspica*, *S. maritima* and *S. eltonica* (Fig. S3). The SSC orientation has been shown to exist in the two different states within individual plants [61–64]. Therefore, SSC variation observed among taxa in this study is likely due to alternative states of the SSC region within individual plants. Although there was some variation in the SSC orientation, the number and content of genes was the same among the eight species. The only exception is the presence of a trnU-TCA in the SSC of *H. ammodendron*.

## Repeat structures and microsatellites

Seven out of the eight chloroplast genomes had 45 to 58 repeats, which ranged in length from 30 to 73 nt per repeat (Fig 1). The majority of these repeats were shown to be between 30 and 40 nt in length. In the *S. eltonica* chloroplast genome, repeat analysis with REPuter [65] found a total of 174 repeats which ranged from 30 to 145 nt in length (Fig 1). The number of repeats was similarly distributed among species for repeats found in intergenic regions and intron/exons (Table 4). An exception was *S. eltonica* in which a majority (80%) of repeats were located in the intergenic regions. Four species possessed reverse repeats; *S. maritima* and *S. aralocaspica* had one, *B. muricata* had two, and *S. eltonica* had four.

The presence of repeats varied for the genes *ycf1*, *ycf2*, *ycf3*, and *psaA*. Repeats were present in the gene *ycf1* except for *A. retroflexus*, *S. aralocaspica* and *S. maritima*. All chloroplast genomes possessed repeats in the *ycf2* gene except for *H. ammodendron*. Repeats in the introns of the *ycf3* gene were only present in the *A. retroflexus*, *B. cycloptera*, and *B. sinuspersici*. All species presented at least one repeat in the *psaA* gene and *H. ammodendron* presented the highest number with six repeats.

Microsatellites, or simple sequence repeats (SSRs), were identified in the eight chloroplast genomes. The total number of microsatellites ranged from 41 to 72 of which the majority, 36 to 64, represent mononucleotide repeat microsatellites (Table 5). The complete list of microsatellites identified for each of the eight chloroplast genomes and their positions in the respective genomes is provided in Table S2.

### **Comparison of *Amaranthus retroflexus* chloroplast genome with previously sequenced *Amaranthus* spp. chloroplast genomes**

*A. retroflexus*, commonly known as pigweed, is used as a vegetable for human consumption as well as for fodder. It is the most widely distributed and damaging *Amaranthus* weed in the US and the world [66]. Availability of the *A. retroflexus* chloroplast genome provides an important tool for accurately monitoring the spread of this species and identifying possible hybridizations. Microsatellites were previously identified for *Amaranthus* spp. [67]. Six out of the nine polymorphic microsatellites were shown to be polymorphic between *A. hypochondriacus* and *A. retroflexus* (Table 6). Most of these microsatellites were located in the LSC regions and represented A or T mononucleotide repeats. SSRs can serve as molecular markers for future molecular breeding for *Amaranthus* spp. which are considered as emerging crops [67]. The chloroplast genomes of four *Amaranthus* spp; *A. hypochondriacus*, *A. cruentus*, *A. caudatus*, and *A. hybridus*, have been reported previously [67]. The *A. hypochondriacus* genome (GenBank accession KX279888.1) is 150,725 nt and the quadripartite regions of LSC, SSC and 2 IRs consist of 83,873, 17,941 and 24,352 nts, respectively. These sizes are very similar to the lengths of the *A. retroflexus* chloroplast genome reported in this study (Table 2). BLAST analysis showed a 99% sequence similarity between the chloroplast genomes of *A. hypochondriacus* and *A. retroflexus*.

### **Comparative analysis of the *B. sinuspersici* chloroplast genomes**

Kim et al. (2016), and Caburatan et al., (2018) previously reported the chloroplast genome of *B. sinuspersici* (GenBank accession no. KU726550). Compared to our results with *B. sinuspersici* (Table 2), the size of their genome (153,472 nt) is 138 nt larger; the LSC and SSC in their study are 84,560 nt and

19,016 nt in size, respectively which is 70 nt larger than in our study (Table 2). The IR was reported to be 24,948 nt in length, versus 24,949 nt length in this study. The increase in length in the published *B. sinuspersici* chloroplast genome [52] is predominantly located at the LSC-IRa and SSC-IRb junctions, which has a repeat of 72 and 13 nts respectively. The two repeats are separated by spacer sequences of 1nt in the LSC-IRa junction and 48 nt in the SSC-IR junction. The 72 and 13 nt sequences were present just once in the *B. sinuspersici* chloroplast genome presented in the current study. The presence of a single occurrence of the 72 and 13 nt sequence in the genome was validated by Sanger sequencing of loci in question for both IRb-LSC and LSC-IRa loci (Table S1). Further comparison of the two *B. sinuspersici* genomes identified 18 SNPs and 9 indels. In the published *B. sinuspersici* chloroplast genome, the LSC is inverted with respect to the rest of the sequence (IRa+SSC+IRb). In our study, the orientation of the LSC was validated using Sanger sequencing of PCR amplicons spanning the junctions IRb-LSC and LSC-IRa (Table S1). As described above, there were also differences in the presence of stop codons in the *rpl23* gene. In the previous study [68] a total of 110 unique genes were reported; a total of a total of 114 genes were identified in the current study (Fig. S3).

Differences between the previously reported chloroplast genome of *B. sinuspersici* compared to the current study likely stems from how the Celera assembler algorithm and the CLC algorithm process the read data. Each of these algorithms have their inherent pros and cons [69]. The assembly parameters for the previous *B. sinuspersici* chloroplast genome were not reported. Also, the chloroplast genome loci that were found to be different within the two previous versions [52,68] were not resequenced. The chloroplast genome of *B. sinuspersici* presented in this study showed a minimum, maximum and average coverage of 37, 23,533, 3,204.28 nt. Furthermore, areas of ambiguity were validated via Sanger sequencing of PCR amplicons generated from selected loci. The combination of the assembly strategy utilized, and resequencing of loci, resulted in the generation of an improved version of the *B. sinuspersici* chloroplast genome.

Analysis of the two closest SCC<sub>4</sub> related species, *B. cycloptera* and *B. sinuspersici*, chloroplast genomes showed a 99.70% sequence similarity between both sequences. *B. cycloptera* and *B. sinuspersici* chloroplast genomes differed in overall length by seven nt. *B. sinuspersici* IR, and SSC regions were larger than the *B. cycloptera* by 44 nt and *B. cycloptera*'s LSC region was larger by 51 nt. The difference in size was due to changes in the intergenic region, length, and number of repeat regions. Number of genes with introns and repeats was the same between the two species. *B. cycloptera* had two larger repeats, one between 40 to 44nt and the second greater than 45nt. *B. sinuspersici* had one smaller repeat of 30 to 34nt. Both species had the same number and identity of protein-coding, tRNA, and rRNA genes.

### **Comparative analysis of *Haloxylon ammodendron* chloroplast genomes: a case of transfer of mitochondrial DNA to the plastid genome**

The chloroplast genome of *H. ammodendron* was published recently (GenBank accession no. KF534478) [70]. The size of the chloroplast genome was reported to be 151,570 nt, with a LSC of 84,214 nt, SSC of 19,014 nt and two IRs of 24,171 nt [70]. In our study, the genome assembled to a size of 161,251 nt,

which is 9,681 nts larger. BLAST alignment of the two genomes indicated that the additional 9,681 nts were derived from the expansion of the IR, which is 4,868 nt in size. The IRs of *H. ammodendron* chloroplast genome in our study were 29,061 nt long. This represents an expansion of the IR that is also observed in *S. eltonica* (Table 2). Expansion and gene duplication are common phenomenon in the IR regions of chloroplast genomes [71,72]. In grasses, the junctions between the IR and SSC regions are highly variable with the ends of genes *ndhF*, *rps19*, and *ndhH* repeatedly migrating into and out of the adjacent IR regions [73]. BLAST alignment between the two genomes revealed that the first 115 nt showed 78% homology with chloroplast sequences of *H. persicum*, and *H. ammodendron* present in the IRs of the published genomes [70]. The following region of 671 nt did not show any significant similarity and the last 4,028 nt showed homology to mitochondrial genome sequences. The highest significant hit (94%; E value = 0.0) for this 4,028 nt section resembled *Beta vulgaris* and *Spinacia oleracea*. Interestingly, annotation identified the mitochondrial gene Cytochrome b (*cob*) in this 4,814 nt section, although the plastid copy had a nonsense mutation that resulted in a premature stop codon.

Evidence showing transfer of mitochondrial DNA (mtDNA) or nuclear DNA (nucDNA) to the plastid genome in plants had been lacking until recently. A few recent reports indicate that plastid genomes of carrot [74], milkweed [75], and bamboo [73] show evidence of gene transfer from mitochondria to the plastid. *Daucus carota* has a 1.5 kb region of mitochondrial origin located in the *rps12-trnV* intergenic space of the chloroplast genome. Only *Daucus* species and the close relative cumin (*Cuminum cyminum*) show the mitochondrion-to-chloroplast gene transfer [74]. It was concluded that a mitochondria-located DNA segment present in the ancestor of the Apiaceae subsequently moved to the plastid genome in the common ancestor of *Daucus* and *Cuminum*. *Asclepias syriaca*, the common milkweed, has a 2.4 kb mtDNA-like insert in the chloroplast genome. The mtDNA-like insert contains an intact exon of the mitochondrial ribosomal protein (*rpl2*) as well as a noncoding region [75]. There was a 92% sequence identity between the mitochondrial and plastid version of *rpl2* in *A. syriaca* whereas the plastid copy had a nonsense mutation resulting in a premature stop codon. Similarly, the IR region in three herbaceous bamboo species of the *Pariana* genus had a 2.7 kb insertion [73]. The insertion was located in the *trnI-CAU-trnL-CAA* intergenic spacer region. Potential variations of this insertion in another *Pariana* species and species from the sister genus *Eremitis* were also reported. These studies suggest that the transferred sequence may have originated as a single event in a common ancestor; however, the inserted sequence evolved rapidly [73].

In our study, the inserted section in *H. ammodendron* had an average coverage of 1,320 x reported from the stringent 0.99-0.99 length fraction/similarity mapped to the assembly. The coverage corresponded well to the average coverage of 1,269 X for other regions. Five kb regions flanking the 4.8kb section had a similar coverage of 929 and 1,066 reads. The Illumina reads from *H. ammodendron* (0.99-0.99 length fraction/similarity fraction) were mapped to three randomly selected intronless mitochondrial genes identified from the *H. ammodendron* assembly [73]. The mitochondrial genes *ccmFN*, *matR* and *rrn26* showed a much lower average coverage of 242, 211, and 447, respectively. Thus, the mapping results supported the result that the insertion in the *H. ammodendron* chloroplast genome was not an artifact of the assembly.

Since the *H. ammodendron* chloroplast genome reported in this study was assembled from reads obtained using total cellular DNA, the origin of 4.8 kb insert was confirmed using a complementary Sanger sequencing approach. Amplified segments flanking the entire 4,814 nt insertion were 6,607, 7,172 and 8,132 nt long with the forward and the reverse primers flanking the *ycf1* and *ndhF* genes, respectively (Fig. 2; Table S3). Primers flanking both the *ycf1* and *ndhF* genes coupled with a primer annealing to the middle section of the inserted region produced amplicons of predicted sizes of 3,810 and 4,458 nt (Fig. 2; Table S3). The PCR results were the first line of confirmation since no PCR amplification should be expected from the published *H. ammodendron* chloroplast genome due to primer mismatch. Interestingly, expected DNA amplicons were also obtained when PCR was performed on *Haloxylon persicum*, a close relative of *H. ammodendron* (Fig. 2). A total section of 6.2 kb, including the 4,814nt inserted section, was sequenced and validated via primer walking (Table S3). The sequenced amplicon results produced a 100% alignment match to the *H. ammodendron* chloroplast genome assembly obtained in this study. Amplification and sequence homology validation of the 4,814 nt section confirmed the presence of the insertion in the *H. ammodendron* chloroplast genome. The integration of intracellularly transferred DNA into the intergenic region of *ycf1* and *ndhF* would be expected as insertion in the coding region would have disrupted gene function.

This is the first report to document mitochondria-to-chloroplast interorganellar gene transfer in the Chenopodiaceae family and the fourth example in angiosperms. However, the mechanisms underlying the transfer of genomic DNA fragments remains to be elucidated [73–75].

### **Chloroplast genomes among different types of C<sub>4</sub> species versus C<sub>3</sub> species**

The 8 chloroplast genomes studied, include the C<sub>3</sub> species *S. maritima* and 7 forms of C<sub>4</sub> species. The results indicate the chloroplast genomes are very similar in the number (82-84) and type of CDS genes encoding proteins. Despite some differences in gene content and organization among the chloroplast genomes, these differences do not coincide with the type of oxygenic photosynthesis (C<sub>3</sub> or C<sub>4</sub>) that these 8 species represent. There is a general conservation of genes present in the C<sub>3</sub> species *B. muricata* and the C<sub>4</sub> species. This suggests nuclear genes encode most chloroplast-targeted proteins that are needed to support the C<sub>4</sub> pathway. Both Kranz type and single-cell type C<sub>4</sub> species have dimorphic chloroplasts (relative to function in carbon assimilation, starch synthesis, and in relative expression of photosystem I and photosystem II for balancing requirements for ATP and NADPH). In carbon assimilation one type of chloroplast supports fixation of atmospheric CO<sub>2</sub> by PEPC with synthesis of C<sub>4</sub> acids. They generate energy to support conversion of pyruvate to phosphoenolpyruvate utilizing pyruvate, Pi dikinase, adenylate kinase, and inorganic pyrophosphatase, and they support reduction of oxaloacetate to malate by NADP-malate dehydrogenase. The other type of chloroplast has the Calvin-Benson cycle with Rubisco fixing CO<sub>2</sub> that is generated by decarboxylation of C<sub>4</sub> acids (utilizing plastid-targeted NADP-malic enzyme in some C<sub>4</sub> species). Currently all enzymes required in chloroplasts to support the C<sub>4</sub> cycle and Calvin-Benson cycle are considered to be nuclear encoded except the gene for the large subunit of Rubisco which is in the chloroplast genome, while the small subunit gene is in the

nucleus [39,76–79]. In the dual-cell Kranz type  $C_4$  plants, cell specific control of transcription of nuclear genes may contribute to development of dimorphic chloroplasts. Other mechanisms must control development of dimorphic chloroplasts in SCC4 species [see hypotheses, selective protein import, selective mRNA targeting, selective protein degradation; [77]]. Future studies are needed to determine how dimorphic chloroplasts develop to coordinate function of  $C_4$  in carbon assimilation, metabolite transport between chloroplasts, and requirements of energy from photochemistry.

## Conclusions

This study reports high quality, and complete chloroplast genomes from seven Chenopodiaceae and one Amaranthaceae species. The procedures show the hybrid method of using high throughput and Sanger sequencing [80,81] is rapid, efficient, and reliable for chloroplast genome sequencing. While genome organization, gene order, and content were largely conserved, there were a few structural differences, such as the variable location of the *ycf15* gene; the high repeat content in the *S. eltonica* genome; the presence of two copies of *ycf1* gene in *H. ammodendron* along with the IR expansion; and the IR expansion in *S. eltonica* that includes the *trnH-GTG* and *psbA*. The biological significance of these differences remains to be investigated.

The *B. sinuspersici* chloroplast genome presented in this study represents an improved version due to the high sequencing coverage and the validation of the junction regions through Sanger sequencing. The improvement in the *B. sinuspersici* chloroplast genome sequence allowed for the identification of a higher number of chloroplast genes. Interestingly, the *H. ammodendron* chloroplast genome presented in this study is 9,681 nt larger than the previously published genome [70]. This difference originated from a duplicated region of the IR, which is 4,868 nt in size and represented a rare instance of interorganellar DNA transfer from the mitochondria to the chloroplast genome.

The purpose of this study was to analyze chloroplast genomes in a few representative dicot species which have different forms of photosynthesis. Due to the high number of variable photosynthetic types present in Chenopodiaceae and almost 90% of the gene products in the chloroplast originating in the nucleus, there may be an expectation that the Chenopodiaceae may include chloroplast-encoded genes corresponding to each photosynthetic phenotype. However, to derive such phylogenetic conclusions requires extensive taxon sampling as exemplified in a recent analysis of 113 grass species [82]. Therefore, such an analysis was outside the purview of the current study.

$C_4$  plants evolved independently from  $C_3$  species more than 60 times [33] leading to development of different forms of Kranz, along with single-cell  $C_4$  species, all of which have dimorphic chloroplasts coordinated in functions to support  $C_4$  photosynthesis. This includes differential expression of enzymes in carbon assimilation, selective expression of metabolite transporters to control flux of carbon between the two chloroplasts, and expression of photosystem I and II for production of ATP and NADPH. How these dimorphic chloroplasts develop through control of expression of nuclear and chloroplast genes remains unknown. Complete chloroplast genomic information on different forms of  $C_4$  species across

dicot and monocot families should be useful in future studies on the control of its development, determining what is required for C<sub>4</sub> photosynthesis, and determining the degree of conservation of the chloroplast genome in these photosynthetic types across phylogeny.

## Materials And Methods

### Plant Material and DNA extraction

*Amaranthus retroflexus*, *Bassia muricata*, *Suaeda eltonica* and *Suaeda maritima* plants were grown in a growth chamber with a 14/10 h photoperiod, light regime of 525 PPFD and day/night, and temperature of 28°C/18°C. The same photoperiod and light regime were used for *Bienertia cycloptera*, *B. sinuspersici* and *Suaeda aralocaspica*; however, the day/night temperatures were modified to 35°C/18°C. *Haloxylon ammodendron* plants were grown under natural annual environmental conditions in Pullman, WA. Total cellular DNA was isolated using fresh leaf tissue from each species with a Urea Lysis Buffer Method. Briefly, leaf tissue was flash frozen in liquid nitrogen and ground to a fine powder and approximately 100 mg tissue was placed in 600 ml buffer containing 42% w/v Urea, 250 mM NaCl, 50 mM Tris (pH 8.0), 1% sodium dodecyl sulfate (SDS) and 20 mM EDTA. Solution was briefly vortexed, extracted with equal volume of 1:1 phenol: chloroform and vortexed for 45 seconds. Samples were then centrifuged at 9,500g for 5 minutes and the supernatant was added to an equal volume of ice cold 2-propanol. The tube was rocked gently six times and centrifuged for 10 minutes at 9,500g. The pellet was washed in 1 mL ice cold 70% ethanol and centrifuged at 9,500g for two minutes and the supernatant was decanted. The pellet was dried and suspended in 500 mL TE buffer with 20 mg/mL RNase A and incubated for 30 minutes at 37°C prior to the addition of 1/10<sup>th</sup> volume 3M sodium acetate (pH 5.3) and 2 volumes of 95% ethanol and rocked gently 6 times. The tube was centrifuged at 9,500g for ten minutes, supernatant removed and the pellet was rinsed with 500 mL 70% ethanol, centrifuged for 2 minutes at 9,500g and the pellet was dried before being suspended in 50 mL TE buffer.

### DNA Sequencing, validation and contig assembly

The paired-end DNA sample prep kit (PE-102-1001; Illumina, San Diego, CA) was used to generate a paired-end library according to manufacturer's recommendations (Illumina, San Diego, CA) at the Research Technology Support Facility at Michigan State University (East Lansing, MI, USA). DNA samples were sequenced on the Illumina HiSeq 2000 utilizing the 100PE chemistry. Quality control on raw sequence data was performed using CLC Genomics Workbench ver. 6.0.1 (CLC), (QIAGEN, Redwood City, CA, USA). CLC was utilized for read trimming, merging reads and filtering out low quality sequences with a phred score below 40. Assembly and mapping of the reads to the contigs was accomplished with CLC software. Mapping of reads to contigs was conducted using the following mapping parameters: mismatch cost 2, insertion cost 3, deletion cost 3, length fraction 0.8 and similarity fraction 0.9. BLASTN searches on NCBI (<https://www.ncbi.nlm.nih.gov/>) were performed using the assembled contigs as query sequences to identify contigs with high homology to chloroplast large single copy (LSC), small single copy (SSC) and inverted repeat (IR) for each of the assembled libraries obtained from each of the eight

plant species. Identified IR contigs were reverse complimented and overlapping borders of each of the identified contigs were aligned to assemble a complete chloroplast genome sequence in the following order of LSC+IR+SSC+IR. Chloroplast contig junctions from overlapping border regions were aligned and analyzed with MEGA6 version 6.0.6 (<http://www.megasoftware.net/>). Flanking primers for chloroplast junctions were designed utilizing Primer 3 Software [83]. PCR amplification was performed using Platinum Taq High-Fidelity DNA polymerase (Invitrogen, CA) and PCR products were purified using the QIAquick PCR purification Kit (QIAGEN, MD). Amplicons, ranging in size from 0.2 to 0.5 kb, were Sanger sequenced to ensure sequence fidelity of the DNA assembly output (Eurofins Genomics, KY). A primer walking and Sanger sequencing method was utilized to identify non-overlapping regions in the LSC+IRa and IRb+LSC junctions of *T. indica* and the IRa+SSC and SSC+IRb junctions of *S. eltonica*. The primer walking and Sanger sequencing method was also employed to validate specific conflicting sequences in the *H. ammodendron* chloroplast genome when compared to the publicly available *H. ammodendron* sequence. A remapping of the Illumina sequenced reads was performed using the final predicted chloroplast genomes from the eight species utilizing CLC software. A length fraction and similarity fraction of 0.99 were chosen as remapping parameters to ensure high stringency alignment. Assemblies generated with 0.80-0.90 and 0.99-0.99 length fraction and similarity fraction were screened to identify regions with coverage below 40x. Sequence data have been deposited to GenBank database under accession numbers MT299584 (*A. retroflexus*), MT316306 (*B. muricata*), MT316305 (*B. cycloptera*), MT316307 (*B. sinuspersici*), MT316308 (*H. ammodendron*), MT316309 (*S. aralocaspica*), MT316310 (*S. eltonica*), and MT316311 (*S. maritima*).

## Genome annotation and Visualization

All the chloroplast genomes were annotated and visualized with GeSeq [43] which incorporates the Dual Organellar Genome Annotator (DOGMA) [44] and OrganellarGenomeDRAW (OGDRAW)[84].

## Comparisons of gene content and gene order

Comparisons for both gene content and order were performed for the eight chloroplast sequences. This comparison included three chloroplast reference genomes: *V. vinifera* (NC\_007957.1), *S. oleracea* (AJ400848.1) and *B. vulgaris* (EF534108.1). Gene order and content were parsed manually using pairwise comparisons between species.

## Examination of repeat structure and microsatellites

REPuter [65] was utilized to identify the number and location of forward, reverse, complementary, and palindromic repeats in the sequence of the eight species predicted chloroplast sequences. A minimum repeat size of 30 nt and a Hamming distance of 3 (>90% sequence identity) was utilized. Shared and unique repeats were identified manually and with the use of BLASTN based on intergenomic comparisons.

Microsatellites were identified with MISA software [85] using standard thresholds. Specifically, a minimum stretch of 10 for mono-, six for di-, five for tri-, and three for tetra-, penta-, and hexa-nucleotide repeats, and a minimum distance of 100 nucleotides between compound microsatellites.

## Declarations

Ethics approval and consent to participate: Not applicable.

Consent for publication: Not applicable.

Availability of data and materials: The sequence of the chloroplast genomes generated during the current study are accessible from GenBank accession numbers: MT299584 (*A. retroflexus*), MT316306 (*B. muricata*), MT316305 (*B. cycloptera*), MT316307 (*B. sinuspersici*), MT316308 (*H. ammodendron*), MT316309 (*S. aralocaspica*), MT316310 (*S. eltonica*), and MT316311 (*S. maritima*), [<https://www.ncbi.nlm.nih.gov/genbank/>]

Competing interests: The authors declare that they have no competing interests.

Funding: Work in the Dhingra lab was supported in part by Washington State University Agriculture Center Research Hatch Grant WNP00011. BWB acknowledges graduate research assistantship support from Washington State University Graduate School.

Authors' contributions: RMS, GEE and AD designed the study. GEE and AD supervised the study. RMS and BWB performed the experiments and generated the data. RMS, BWB and AD analyzed the data. All authors read and approved the final manuscript.

Acknowledgements: The authors acknowledge Sequoia Dance for her support with PCR.

## Bibliography

1. Neuhaus HE, Emes MJ. Nonphotosynthetic metabolism in plastids. *Annu Rev Plant Physiol Plant Mol Biol* [Internet]. 2000;51:111–40. Available from: <http://www.annualreviews.org/doi/abs/10.1146/annurev.arplant.51.1.111>
2. Namitha KK, Negi PS. Chemistry and Biotechnology of Carotenoids. *Crit Rev Food Sci Nutr* [Internet]. 2010;50:728–60. Available from: <http://www.tandfonline.com/doi/abs/10.1080/10408398.2010.499811>
3. Jansen RK, Cai Z, Raubeson LA, Daniell H, Depamphilis CW, Leebens-Mack J, et al. Analysis of 81 genes from 64 plastid genomes resolves relationships in angiosperms and identifies genome-scale evolutionary patterns. *Proc Natl Acad Sci. National Acad Sciences*; 2007;104:19369–74.
4. Shaw J, Lickey EB, Schilling EE, Small RL. Comparison of whole chloroplast genome sequences to choose noncoding regions for phylogenetic studies in angiosperms: the tortoise and the hare III. *Am J Bot. Wiley Online Library*; 2007;94:275–88.

5. Green BR. Chloroplast genomes of photosynthetic eukaryotes. *Plant J* [Internet]. 2011;66:34–44. Available from: <http://doi.wiley.com/10.1111/j.1365-313X.2011.04541.x>
6. Svab Z, Hajdukiewicz P, Maliga P. Stable transformation of plastids in higher plants. *Proc Natl Acad Sci. National Acad Sciences*; 1990;87:8526–30.
7. Dhingra A, Daniell H. Chloroplast genetic engineering via organogenesis or somatic embryogenesis. *Arab Protoc. Springer*; 2006. p. 245–62.
8. Palmer JD, Osorio B, Aldrich J, Thompson WF. Chloroplast DNA evolution among legumes: Loss of a large inverted repeat occurred prior to other sequence rearrangements. *Curr Genet* [Internet]. 1987;11:275–86. Available from: <https://doi.org/10.1007/BF00355401>
9. Wu C-S, Chaw S-M. Large-Scale Comparative Analysis Reveals the Mechanisms Driving Plastomic Compaction, Reduction, and Inversions in Conifers II (Cupressophytes). *Genome Biol Evol* [Internet]. 2016;evw278. Available from: <https://academic.oup.com/gbe/article-lookup/doi/10.1093/gbe/evw278>
10. Braukmann TWA, Broe MB, Stefanović S, Freudenstein J V. On the brink: the highly reduced plastomes of nonphotosynthetic Ericaceae. *New Phytol* [Internet]. 2017;216:254–66. Available from: <http://doi.wiley.com/10.1111/nph.14681>
11. Dhingra A, Folta KM. ASAP: amplification, sequencing & annotation of plastomes. *BMC Genomics. BioMed Central*; 2005;6:176.
12. Cahoon AB, Sharpe RM, Mysayphonh C, Thompson EJ, Ward AD, Lin A. The complete chloroplast genome of tall fescue (*Lolium arundinaceum*; Poaceae) and comparison of whole plastomes from the family Poaceae. *Am J Bot* [Internet]. 2010;97:49–58. Available from: <http://www.amjbot.org/cgi/content/abstract/97/1/49>
13. Zhang Y-J, Ma P-F, Li D-Z. High-Throughput Sequencing of Six Bamboo Chloroplast Genomes: Phylogenetic Implications for Temperate Woody Bamboos (Poaceae: Bambusoideae). Poon AFY, editor. *PLoS One* [Internet]. 2011;6:e20596. Available from: <http://dx.plos.org/10.1371/journal.pone.0020596>
14. Wu J, Liu B, Cheng F, Ramchiary N, Choi SR, Lim YP, et al. Sequencing of Chloroplast Genome Using Whole Cellular DNA and Solexa Sequencing Technology. *Front Plant Sci* [Internet]. 2012;3. Available from: [http://www.frontiersin.org/Plant\\_Genetics\\_and\\_Genomics/10.3389/fpls.2012.00243/abstract](http://www.frontiersin.org/Plant_Genetics_and_Genomics/10.3389/fpls.2012.00243/abstract)
15. Moore MJ, Dhingra A, Soltis PS, Shaw R, Farmerie WG, Folta KM, et al. Rapid and accurate pyrosequencing of angiosperm plastid genomes. *BMC Plant Biol. BioMed Central*; 2006;6:17.
16. Nagy E, Hegedűs G, Taller J, Kutasy B, Virág E. Illumina sequencing of the chloroplast genome of common ragweed (*Ambrosia artemisiifolia* L.). *Data Br. Elsevier*; 2017;15:606–11.
17. Sakaguchi S, Ueno S, Tsumura Y, Setoguchi H, Ito M, Hattori C, et al. Application of a simplified method of chloroplast enrichment to small amounts of tissue for chloroplast genome sequencing. *Appl Plant Sci. Wiley Online Library*; 2017;5:1700002.
18. Sakulsathaporn A, Wonnapijit P, Vuttipongchaikij S, Apisitwanich S. The complete chloroplast genome sequence of Asian Palmyra palm (*Borassus flabellifer*). *BMC Res Notes. BioMed Central*;

2017;10:740.

19. Keller J, Rousseau-Gueutin M, Martin GE, Morice J, Boutte J, Coissac E, et al. The evolutionary fate of the chloroplast and nuclear rps16 genes as revealed through the sequencing and comparative analyses of four novel legume chloroplast genomes from *Lupinus*. *Dna Res*. Oxford University Press; 2017;24:343–58.
20. Schuster TM, Setaro SD, Tibbits JFG, Batty EL, Fowler RM, McLay TGB, et al. Chloroplast variation is incongruent with classification of the Australian bloodwood eucalypts (genus *Corymbia*, family Myrtaceae). *PLoS One*. Public Library of Science; 2018;13:e0195034.
21. Nock CJ, Hardner CM, Montenegro JD, Termizi AAA, Hayashi S, Playford J, et al. Wild origins of macadamia domestication identified through intraspecific chloroplast genome sequencing. *Front Plant Sci*. Frontiers; 2019;10:334.
22. Dong W, Xu C, Cheng T, Lin K, Zhou S. Sequencing Angiosperm Plastid Genomes Made Easy: A Complete Set of Universal Primers and a Case Study on the Phylogeny of Saxifragales. *Genome Biol Evol* [Internet]. 2013;5:989–97. Available from: <https://academic.oup.com/gbe/article-lookup/doi/10.1093/gbe/evt063>
23. Logacheva MD, Samigullin TH, Dhingra A, Penin AA. Comparative chloroplast genomics and phylogenetics of *Fagopyrum esculentum* ssp. *ancestrale*—a wild ancestor of cultivated buckwheat. *BMC Plant Biol*. BioMed Central; 2008;8:59.
24. Wang R-J, Cheng C-L, Chang C-C, Wu C-L, Su T-M, Chaw S-M. Dynamics and evolution of the inverted repeat-large single copy junctions in the chloroplast genomes of monocots. *BMC Evol Biol* [Internet]. 2008;8:36. Available from: <http://bmcevolbiol.biomedcentral.com/articles/10.1186/1471-2148-8-36>
25. Peng L, Yamamoto H, Shikanai T. Structure and biogenesis of the chloroplast NAD (P) H dehydrogenase complex. *Biochim Biophys Acta (BBA)-Bioenergetics*. Elsevier; 2011;1807:945–53.
26. Gu C, Tembrock LR, Li Y, Lu X, Wu Z. The complete chloroplast genome of queen's crape-myrtle (*Lagerstroemia macrocarpa*). *Mitochondrial DNA Part B*. Taylor & Francis; 2016;1:408–9.
27. Weng M-L, Ruhlman TA, Jansen RK. Expansion of inverted repeat does not decrease substitution rates in *Pelargonium* plastid genomes. *New Phytol* [Internet]. 2017;214:842–51. Available from: <http://doi.wiley.com/10.1111/nph.14375>
28. Zuo L-H, Shang A-Q, Zhang S, Yu X-Y, Ren Y-C, Yang M-S, et al. The first complete chloroplast genome sequences of *Ulmus* species by de novo sequencing: Genome comparative and taxonomic position analysis. Chen S, editor. *PLoS One* [Internet]. 2017;12:e0171264. Available from: <http://dx.plos.org/10.1371/journal.pone.0171264>
29. Jurić I, González-Pérez V, Hibberd JM, Edwards G, Burroughs NJ. Size matters for single-cell C4 photosynthesis in *Bienertia*. *J Exp Bot* [Internet]. 2016; Available from: <http://jxb.oxfordjournals.org/content/early/2016/10/12/jxb.erw374.abstract>
30. Offermann S, Friso G, Doroshenk KA, Sun Q, Sharpe RM, Okita TW, et al. Developmental and Subcellular Organization of Single-Cell C4 Photosynthesis in *Bienertia sinuspersici* Determined by

- Large-Scale Proteomics and cDNA Assembly from 454 DNA Sequencing. *J Proteome Res* [Internet]. 2015;14:2090–108. Available from: <http://pubs.acs.org/doi/abs/10.1021/pr5011907>
31. Edwards GE, Franceschi VR, Voznesenskaya E V. SINGLE-CELL C 4 PHOTOSYNTHESIS VERSUS THE DUAL-CELL (KRANZ) PARADIGM. *Annu Rev Plant Biol* [Internet]. 2004;55:173–96. Available from: <http://www.annualreviews.org/doi/abs/10.1146/annurev.arplant.55.031903.141725>
  32. Voznesenskaya E V, Franceschi VR, Kiirats O, Artyusheva EG, Freitag H, Edwards GE. Proof of C4 photosynthesis without Kranz anatomy in *Bienertia cycloptera* (Chenopodiaceae). *Plant J* [Internet]. 2002;31:649–62. Available from: <http://doi.wiley.com/10.1046/j.1365-313X.2002.01385.x>
  33. Sage RF, Christin P-A, Edwards EJ. The C4 plant lineages of planet Earth. *J Exp Bot* [Internet]. 2011;62:3155–69. Available from: <http://jxb.oxfordjournals.org/content/62/9/3155.abstract>
  34. Hernández-Ledesma P, Berendsohn WG, Borsch T, Von Mering S, Akhani H, Arias S, et al. A taxonomic backbone for the global synthesis of species diversity in the angiosperm order Caryophyllales. *Willdenowia*. JSTOR; 2015;281–383.
  35. Edwards GE, Voznesenskaya E V. Chapter 4 C4 Photosynthesis: Kranz Forms and Single-Cell C4 in Terrestrial Plants. 2010. p. 29–61.
  36. Kadereit G, Borsch T, Weising K, Freitag H. Phylogeny of Amaranthaceae and Chenopodiaceae and the Evolution of C 4 Photosynthesis. *Int J Plant Sci* [Internet]. 2003;164:959–86. Available from: <http://www.jstor.org/stable/10.1086/378649>
  37. Schütze P, Freitag H, Weising K. An integrated molecular and morphological study of the subfamily Suaedoideae Ulbr. (Chenopodiaceae). *Plant Syst Evol* [Internet]. 2003;239:257–86. Available from: <http://link.springer.com/10.1007/s00606-003-0013-2>
  38. Kapralov M V, Akhani H, Voznesenskaya E V, Edwards G, Franceschi V, Roalson EH. Phylogenetic Relationships in the Salicornioideae / Suaedoideae / Salsoloideae s.l. (Chenopodiaceae) Clade and a Clarification of the Phylogenetic Position of *Bienertia* and *Alexandra* Using Multiple DNA Sequence Datasets. *Syst Bot* [Internet]. 2006;31:571–85. Available from: <http://www.bioone.org/doi/abs/10.1043/06-01.1>
  39. Sharpe RM, Offermann S. One decade after the discovery of single-cell C4 species in terrestrial plants: what did we learn about the minimal requirements of C4 photosynthesis? *Photosynth Res* [Internet]. 2014;119:169–80. Available from: <http://link.springer.com/10.1007/s11120-013-9810-9>
  40. Sage RF. The evolution of C4 photosynthesis. *New Phytol* [Internet]. 2004;161:341–70. Available from: <http://dx.doi.org/10.1111/j.1469-8137.2004.00974.x>
  41. Christin P-A, Sage TL, Edwards EJ, Ogburn RM, Khoshravesh R, Sage RF. COMPLEX EVOLUTIONARY TRANSITIONS AND THE SIGNIFICANCE OF C3–C4 INTERMEDIATE FORMS OF PHOTOSYNTHESIS IN MOLLUGINACEAE. *Evolution (N Y)* [Internet]. 2011;65:643–60. Available from: <http://dx.doi.org/10.1111/j.1558-5646.2010.01168.x>
  42. Altschul SF, Gish W, Miller W, Myers EW, Lipman DJ. Basic local alignment search tool. *J Mol Biol*. Elsevier; 1990;215:403–10.

43. Tillich M, Lehwark P, Pellizzer T, Ulbricht-Jones ES, Fischer A, Bock R, et al. GeSeq—versatile and accurate annotation of organelle genomes. *Nucleic Acids Res. Oxford University Press*; 2017;45:W6–11.
44. Wyman SK, Jansen RK, Boore JL. Automatic annotation of organellar genomes with DOGMA. *Bioinformatics [Internet]*. 2004;20:3252–5. Available from: <http://bioinformatics.oxfordjournals.org/content/20/17/3252.abstract>
45. Chen Y-C, Liu T, Yu C-H, Chiang T-Y, Hwang C-C. Effects of GC bias in next-generation-sequencing data on de novo genome assembly. *PLoS One. Public Library of Science*; 2013;8:e62856.
46. Rieber N, Zapatka M, Lasitschka B, Jones D, Northcott P, Hutter B, et al. Coverage bias and sensitivity of variant calling for four whole-genome sequencing technologies. *PLoS One. Public Library of Science*; 2013;8:e66621.
47. Sims D, Sudbery I, Illott NE, Heger A, Ponting CP. Sequencing depth and coverage: key considerations in genomic analyses. *Nat Rev Genet [Internet]*. 2014;15:121–32. Available from: <http://www.nature.com/articles/nrg3642>
48. Lindsey RL, Pouseele H, Chen JC, Strockbine NA, Carleton HA. Implementation of whole genome sequencing (WGS) for identification and characterization of Shiga toxin-producing *Escherichia coli* (STEC) in the United States. *Front Microbiol. Frontiers*; 2016;7:766.
49. Raubeson LA, Peery R, Chumley TW, Dziubek C, Fourcade HM, Boore JL, et al. Comparative chloroplast genomics: analyses including new sequences from the angiosperms *Nuphar advena* and *Ranunculus macranthus*. *BMC Genomics. BioMed Central*; 2007;8:174.
50. Park J-S, Choi I-S, Lee D-H, Choi B-H. The complete plastid genome of *Suaeda malacosperma* (Amaranthaceae/Chenopodiaceae), a vulnerable halophyte in coastal regions of Korea and Japan. *Mitochondrial DNA Part B. Taylor & Francis*; 2018;3:382–3.
51. Kim Y, Park J, Chung Y. The complete chloroplast genome of *Suaeda japonica* Makino (Amaranthaceae). *Mitochondrial DNA Part B. Taylor & Francis*; 2019;4:1505–7.
52. Kim B, Kim J, Park H, Park J. The complete chloroplast genome sequence of *Bienertia sinuspersici*. *Mitochondrial DNA Part B. Taylor & Francis*; 2016;1:388–9.
53. Yang M, Zhang X, Liu G, Yin Y, Chen K, Yun Q, et al. The complete chloroplast genome sequence of date palm (*Phoenix dactylifera* L.). *PLoS One. Public Library of Science*; 2010;5:e12762.
54. Firetti F, Zuntini AR, Gaiarsa JW, Oliveira RS, Lohmann LG, Van Sluys M. Complete chloroplast genome sequences contribute to plant species delimitation: A case study of the *Anemopaegma* species complex. *Am J Bot. Wiley Online Library*; 2017;104:1493–509.
55. Fonseca LHM, Lohmann LG. Plastome rearrangements in the “*Adenocalymma-Neojobertia*” Clade (Bignoniaceae, Bignoniaceae) and its phylogenetic implications. *Front Plant Sci. Frontiers*; 2017;8:1875.
56. Kim K-J, Lee H-L. Complete chloroplast genome sequences from Korean ginseng (*Panax schinseng* Nees) and comparative analysis of sequence evolution among 17 vascular plants. *DNA Res. Oxford University Press*; 2004;11:247–61.

57. Dong W, Liu J, Yu J, Wang L, Zhou S. Highly variable chloroplast markers for evaluating plant phylogeny at low taxonomic levels and for DNA barcoding. *PLoS One*. Public Library of Science; 2012;7:e35071.
58. Qian J, Song J, Gao H, Zhu Y, Xu J, Pang X, et al. The complete chloroplast genome sequence of the medicinal plant *Salvia miltiorrhiza*. *PLoS One*. Public Library of Science; 2013;8:e57607.
59. Asaf S, Khan AL, Khan AR, Waqas M, Kang S-M, Khan MA, et al. Complete chloroplast genome of *Nicotiana otophora* and its comparison with related species. *Front Plant Sci*. Frontiers; 2016;7:843.
60. Downie SR, Olmstead RG, Zurawski G, Soltis DE, Soltis PS, Watson JC, et al. Six independent losses of the chloroplast DNA *rpl2* intron in dicotyledons: molecular and phylogenetic implications. *Evolution (N Y)*. Wiley Online Library; 1991;45:1245–59.
61. Palmer JD. Chloroplast DNA exists in two orientations. *Nature*. Nature Publishing Group; 1983;301:92–3.
62. Oldenburg DJ, Bendich AJ. Most chloroplast DNA of maize seedlings in linear molecules with defined ends and branched forms. *J Mol Biol*. Elsevier; 2004;335:953–70.
63. Martin G, Baurens F-C, Cardi C, Aury J-M, D'Hont A. The complete chloroplast genome of banana (*Musa acuminata*, Zingiberales): insight into plastid monocotyledon evolution. *PLoS One*. Public Library of Science; 2013;8:e67350.
64. Walker JF, Zanis MJ, Emery NC. Correction to “Comparative analysis of complete chloroplast genome sequence and inversion variation in *Lasthenia burkei* (Madieae, Asteraceae).” *Am J Bot*. Wiley Online Library; 2015;102:1008.
65. Kurtz S, Choudhuri J V, Ohlebusch E, Schleiermacher C, Stoye J, Giegerich R. REPuter: the manifold applications of repeat analysis on a genomic scale. *Nucleic Acids Res*. Oxford University Press; 2001;29:4633–42.
66. Tranel PJ, Trucco F. 21st-century weed science: a call for *Amaranthus* genomics. *Weedy and invasive plant genomics*. Wiley Online Library; 2009;53–81.
67. Chaney L, Mangelson R, Ramaraj T, Jellen EN, Maughan PJ. The complete chloroplast genome sequences for four *Amaranthus* species (Amaranthaceae). *Appl Plant Sci*. 2016;4:1–6.
68. Caburatan L, Kim JG, Park J. Comparative Chloroplast Genome Analysis of Single-Cell C4 *Bienertia Sinuspersici* with Other *Amaranthaceae* Genomes. *J Plant Sci*. Science Publishing Group; 2018;6:134–43.
69. Li Z, Chen Y, Mu D, Yuan J, Shi Y, Zhang H, et al. Comparison of the two major classes of assembly algorithms: overlap–layout–consensus and de-bruijn-graph. *Brief Funct Genomics*. Oxford University Press; 2012;11:25–37.
70. Dong W, Xu C, Li D, Jin X, Li R, Lu Q, et al. Comparative analysis of the complete chloroplast genome sequences in psammophytic *Haloxylon* species (Amaranthaceae). *PeerJ [Internet]*. 2016;4:e2699. Available from: <https://peerj.com/articles/2699>
71. Goulding SE, Wolfe KH, Olmstead RG, Morden CW. Ebb and flow of the chloroplast inverted repeat. *Mol Gen Genet MGG*. Springer; 1996;252:195–206.

72. Lee S-B, Kaittanis C, Jansen RK, Hostetler JB, Tallon LJ, Town CD, et al. The complete chloroplast genome sequence of *Gossypium hirsutum*: organization and phylogenetic relationships to other angiosperms. *BMC Genomics*. BioMed Central; 2006;7:61.
73. Ma P-F, Zhang Y-X, Guo Z-H, Li D-Z. Evidence for horizontal transfer of mitochondrial DNA to the plastid genome in a bamboo genus. *Sci Rep*. Nature Publishing Group; 2015;5:11608.
74. Iorizzo M, Grzebelus D, Senalik D, Szklarczyk M, Spooner D, Simon P. Against the traffic: the first evidence for mitochondrial DNA transfer into the plastid genome. *Mob Genet Elements*. Taylor & Francis; 2012;2:261–6.
75. Straub SCK, Cronn RC, Edwards C, Fishbein M, Liston A. Horizontal transfer of DNA from the mitochondrial to the plastid genome and its subsequent evolution in milkweeds (Apocynaceae). *Genome Biol Evol*. Oxford University Press; 2013;5:1872–85.
76. Wimmer D, Bohnhorst P, Shekhar V, Hwang I, Offermann S. Transit peptide elements mediate selective protein targeting to two different types of chloroplasts in the single-cell C4 species *Bienertia sinuspersici*. *Sci Rep* [Internet]. 2017;7:41187. Available from: <http://www.nature.com/articles/srep41187>
77. Offermann S, Okita TW, Edwards GE. Resolving the compartmentation and function of C4 photosynthesis in the single-cell C4 species *Bienertia sinuspersici*. *Plant Physiol*. *Plant Physiol*; 2011;155:1612–28.
78. Hibberd JM, Covshoff S. The Regulation of Gene Expression Required for C4 Photosynthesis. *Annu Rev Plant Biol* [Internet]. 2010;61:181–207. Available from: <http://www.annualreviews.org/doi/abs/10.1146/annurev-arplant-042809-112238>
79. Dhingra A, Portis Jr. AR, Daniell H. Enhanced translation of a chloroplast-expressed RbcS gene restores small subunit levels and photosynthesis in nuclear RbcS antisense plants. *Proc Natl Acad Sci U S A*. 2004;101.
80. Twyford AD, Ness RW. Strategies for complete plastid genome sequencing. *Mol Ecol Resour*. Wiley Online Library; 2017;17:858–68.
81. Wang W, Schalamun M, Morales-Suarez A, Kainer D, Schwessinger B, Lanfear R. Assembly of chloroplast genomes with long-and short-read data: a comparison of approaches using *Eucalyptus pauciflora* as a test case. *BMC Genomics*. BioMed Central; 2018;19:977.
82. Piot A, Hackel J, Christin PA, Besnard G. One-third of the plastid genes evolved under positive selection in PACMAD grasses. *Planta*. Springer Verlag; 2018;247:255–66.
83. Untergasser A, Cutcutache I, Koressaar T, Ye J, Faircloth BC, Remm M, et al. Primer3—new capabilities and interfaces. *Nucleic Acids Res*. Oxford University Press; 2012;40:e115–e115.
84. Greiner S, Lehwark P, Bock R. OrganellarGenomeDRAW (OGDRAW) version 1.3.1: expanded toolkit for the graphical visualization of organellar genomes. *Nucleic Acids Res* [Internet]. 2019;47:W59–64. Available from: <https://doi.org/10.1093/nar/gkz238>
85. Beier S, Thiel T, Münch T, Scholz U, Mascher M. MISA-web: a web server for microsatellite prediction. *Bioinformatics*. Oxford University Press; 2017;33:2583–5.

## Tables

Please see the supplementary files section to view the tables.

## Figures

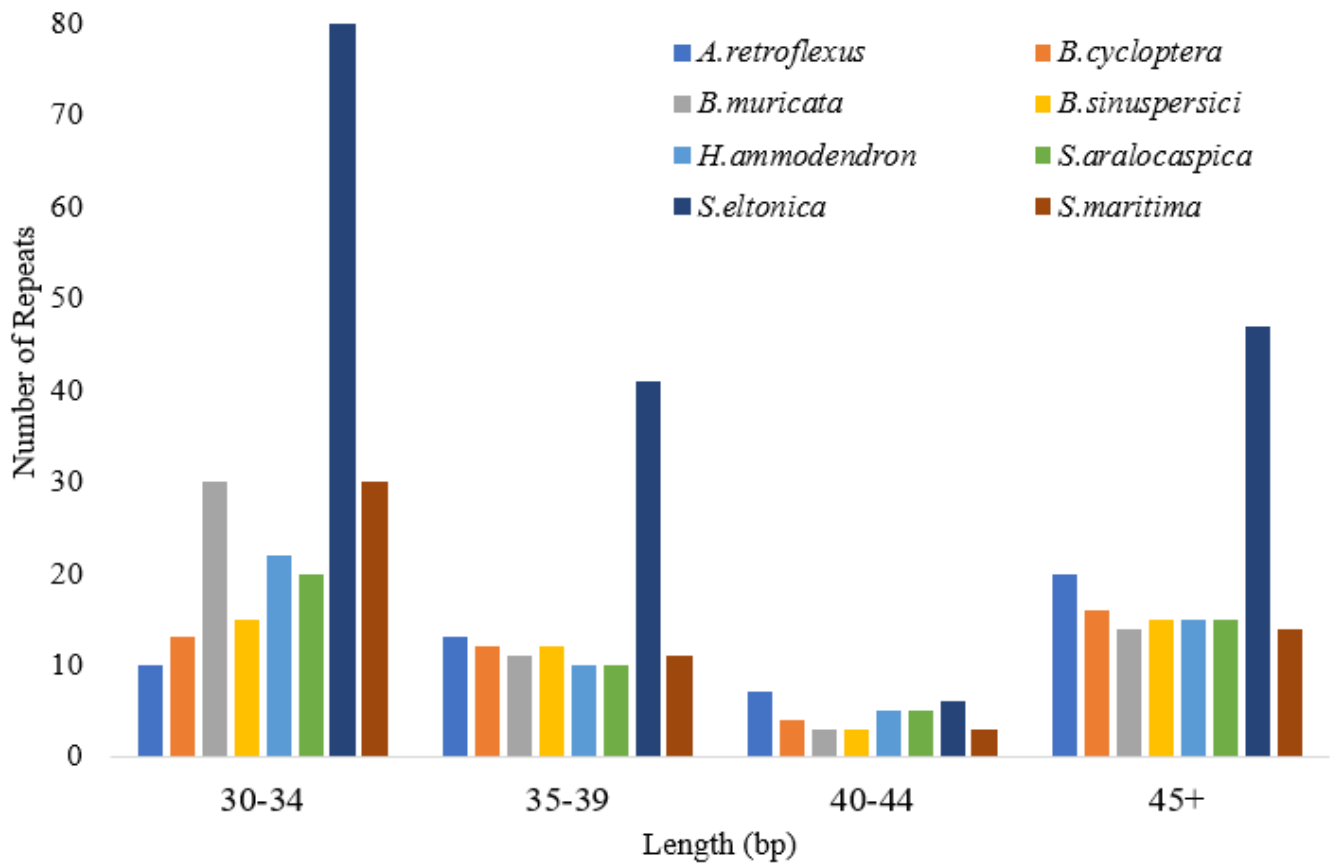


**Figure 1**

Histogram of number of repeated sequences (>30 nt) in length identified with REPuter for nine chloroplast genomes. .

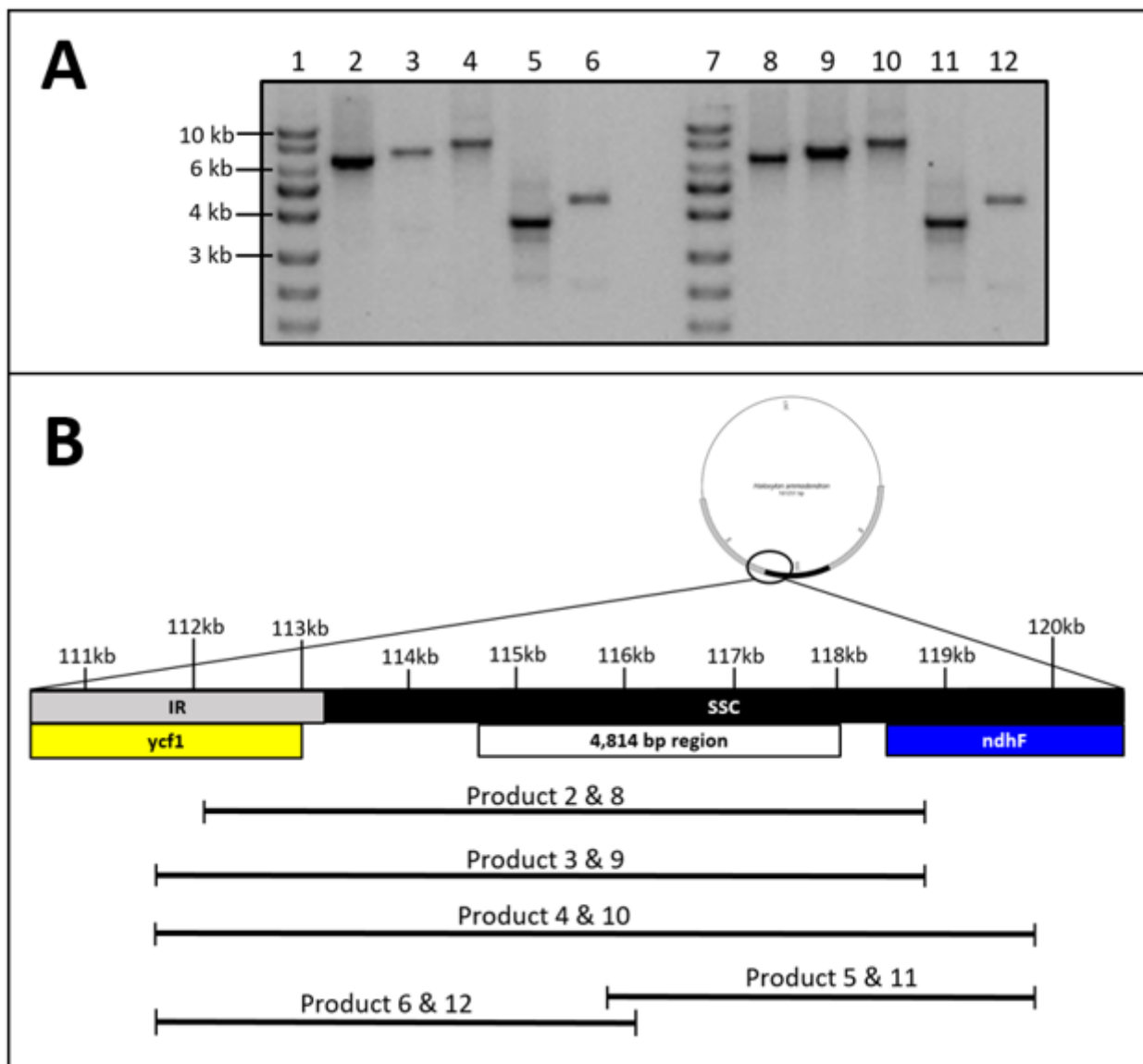


**Figure 2**

PCR amplicons flanking a 4.8kb insertion in the chloroplast genome of *H. ammodendron* (2 to 6) and *H. persicum* (8 to 12). Agarose gel electrophoresis of PCR products (A); diagram representing location and length of each amplicon (B). Expected amplicon sizes are 6607 (2 and 8), 7172 (3 and 9), 8132 (4 and 6), 3810 (5 and 11), and 4458 nt (6 and 12). Primers for PCRs 2 to 4 and 8 to 10 flank the *ycf1* and *ndhF* genes. Primers for PCRs 5 and 11 flank the middle section of the 4.8 kb insertion and the *ndhF* gene. Primers for PCRs 6 and 12 flank the *ycf1* gene and the middle section of the 4.8 kb insertion. 1 and 7: exACTGene DNA Ladders 1kb DNA Ladder..

## Supplementary Files

This is a list of supplementary files associated with this preprint. Click to download.

- [SupplementaryFigure1.pptx](#)

- SupplementaryFigure2.pptx
- SupplementaryFigure3.pptx
- SupplementaryTable1.pptx
- SupplementaryTable2.pptx
- SupplementaryTable3.xlsx
- Table1.pptx
- Table2.pptx
- Table3.pptx
- Table4.pptx
- Table5.xlsx
- Table6.xlsx